Dipole active rotations of physisorbed H_2 and D_2

K. Svensson, J. Bellman, A. Hellman, and S. Andersson
Department of Applied Physics, Chalmers University of Technology and Göteborg University, SE-412 96 Göteborg, Sweden
(Received 11 November 2004; published 2 June 2005)

We have, in electron-energy-loss measurements, observed dipole activity associated with the $j=0\rightarrow 2$ rotational transitions for H_2 and D_2 physisorbed on a Cu(100) surface and at Au adatoms on this surface. Such dipole transitions, which are forbidden for the free molecules, provide for example, via rotation-translation conversion, channels for infrared photodesorption. Using two simple dipole moment functions, we have, for the bare Cu(100) surface, calculated dipole matrix elements for the rotational transition and its combination mode with the $\nu=0\rightarrow 1$ vibrational transition in the physisorption well. Our calculations reveal that the anisotropy of the molecular electronic polarizability induces a significant dynamic dipole coupled to the rotational and rotational-vibrational motion, but are unable to reproduce the measured relative intensities of the corresponding transitions.

DOI: 10.1103/PhysRevB.71.245402 PACS number(s): 67.70.+n, 68.43.Pq, 79.20.Uv

I. INTRODUCTION

In a study in progress, we have found that clusters of H_2 and D_2 preferentially adsorb at Cu and Au adatoms deposited on a cold Cu(100) surface.[1] Electron-energy-loss spectroscopy (EELS) shows that the molecules are physically adsorbed but with a particular and revealing signature: the $j=0\rightarrow 2$ rotational transition is dipole active, while such activity for the free molecule is forbidden. Pure rotational dipole activity for molecules adsorbed on the bare Cu(100) surface is too weak to be detected, and we have used this difference to discriminate between molecules decorating the Cu and Au monomers and those adsorbed on the bare Cu(100) surface. However, the EELS measurements for H_2 and D_2 adsorbed on the bare Cu(100) surface show relatively intense dipole active combination modes involving the $j=0\rightarrow 2$ rotational and the $\nu=0\rightarrow 1$ vibrational transition in the physisorption well. This observation implies that the rotation must have a finite dipole cross section also in the bare surface case. In order to understand the physical origin of this dipole excitation mechanism, we have measured the dipole contributions and evaluated the relevant dipole matrix elements. The experimental observations have been compared with calculated dipole matrix elements for different contributions to the dipole moment function of the physisorbed molecule.

A permanent dipole, which depends on the molecular electronic polarizability α, will be induced in the physisorbed molecule.[2,3] Rotational anisotropy of α, which causes the Raman activity of the $j=0\rightarrow 2$ rotational transition of a free homonuclear molecule like H_2,[4] induces a fluctuating dipole in a rotating physisorbed H_2 molecule and hence a dipole-active $j=0\rightarrow 2$ transition. Similarly, the $n=0\rightarrow 1$ internal vibration, which is Raman active for free H_2 because α depends on the molecular bond length,[4] will also be dipole active in the physisorption situation.[5] Regarding H_2 physisorbed on Cu(100), we find, in our calculations, that the rotational anisotropy of α causes a significant dipole activity in both the $j=0\rightarrow 2$ rotational mode and the $j=0\rightarrow 2$, $\nu=0\rightarrow 1$ combination mode. The calculated dipole matrix elements for the combination mode are, however, considerably weaker than the measured values and the relative trend of the calculated values for the rotation and rotation-vibration modes is opposite to the measured data. In this context, we note that these relatively intense dipole transitions provide, via rotation-translation conversion, channels for infrared photodesorption complementary to the direct channels involving dipole active transitions from the ground state to continuum states of the physisorption well.[6] The experimental data also show that proximity to a Au adatom increases the $j=0\rightarrow 2$ rotational dipole activity drastically. For example, for D_2 the measured dipole matrix element is about an order of magnitude larger than the calculated value for D_2 physisorbed on the bare Cu(100) surface.

II. EXPERIMENT

The spectroscopic measurements reported here were carried out with use of a high-resolution electron-energy-loss spectrometer (EELS). The spectrometer, which is an improved version of a construction that has been described briefly elsewhere,[7] has an optimum energy resolution of about 1 meV. The electron analyzer and the specimen can be rotated so that the angles of incident and detected electrons can be varied independently. Angular distribution measurements were obtained by rotating the analyzer. The x-ray aligned ($<0.2°$) and polished Cu(100) surface was cleaned *in situ* by standard methods involving argon-ion bombardment and heating cycles and could be cooled, at an ambient pressure in the 10^{-11} Torr range, to temperatures around 10 K using helium as a cryogen. Prior to hydrogen adsorption, the specimen was flash-heated to 900 K and rapidly cooled to 10 K. EELS spectra were taken for uncompressed monolayers of physisorbed H_2 and D_2 of approximately equal adsorbate density determined to be around 0.7×10^{15} molecules/cm^2 in previous desorption experiments.[8] The adsorbate density was routinely monitored by work-function measurements, for example, an uncompressed full H_2 monolayer causes a reduction of the work function, $\Delta\Phi=-0.12$ eV.[8]

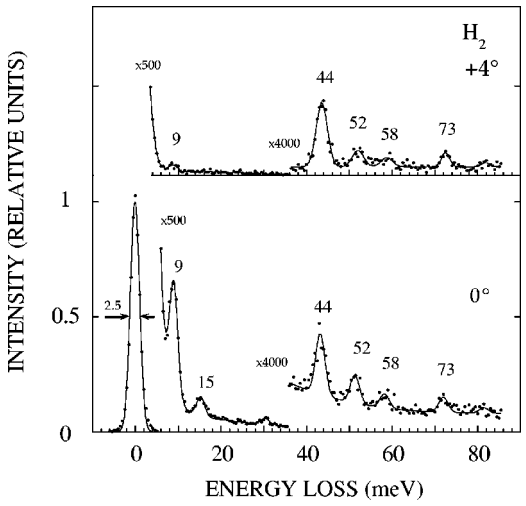

FIG. 1. In (0°) and off (+4°) specular EELS spectra of an uncompressed monolayer of H_2 adsorbed on a 10 K Cu(100) surface. Both spectra are normalized to the specular elastic peak and were obtained for a 3 eV electron beam incident at 48° from the surface normal.

Figure 1 shows EELS spectra obtained in the specular (0°) and off-specular (+4°) directions for a monolayer of adsorbed H_2. The low-energy peaks at 9 and 15 meV correspond to the $\nu=0\rightarrow1$ and $\nu=0\rightarrow2$ vibrational transitions in the physisorption well. These modes are dipole excited and the spectral intensity peaks sharply in the specular direction. A detailed discussion of this spectral range has been presented elsewhere.[9] The peaks at 44, 52, and 58 meV are due to the $j=0\rightarrow2$ rotational excitation and its combination modes with the $\nu=0\rightarrow1$ and $\nu=0\rightarrow2$ vibrational transitions. While the dipole-excited low-energy peaks and the background due to dipole-excited electron-hole pairs[10] fall off rapidly in intensity away from the specular direction, the pure rotational peak persists, a characteristic behaviour for short-range inelastic scattering. Figure 2 shows angular distribution measurements for H_2 of the specular elastic peak, the $j=0\rightarrow2$ peak and the $j=0\rightarrow2$, $\nu=0\rightarrow1$ peak. The pure rotation exhibits a broad smooth distribution while the combination mode shows a dipole-excited specular distribution superimposed on a broad short-range scattering distribution. Dipole excitation of the combination mode implies that the pure rotation must have a finite dipole contribution but the flat angular distribution of the pure rotation shows that this contribution is clearly weaker than for the combination mode.

Figure 2 also shows corresponding experimental data for HD, $j=0\rightarrow2$ at 33 meV and $j=0\rightarrow2$, $\nu=0\rightarrow1$ at 40 meV and D_2, $j=0\rightarrow2$ at 22 meV and $j=0\rightarrow2$, $\nu=0\rightarrow1$ at 29 meV. The data are qualitatively similar to those for H_2; flat distributions for the $j=0\rightarrow2$ rotation and a dipole-excited specular distribution superimposed on a broad short-range scattering distribution for the $j=0\rightarrow2$, $\nu=0\rightarrow1$ combination mode. We have obtained the dipole contribution of the $j=0\rightarrow2$, $\nu=0\rightarrow1$ transition by subtracting off a constant short-range background as shown by the dashed curves in Fig. 2. It is straightforward to evaluate dipole matrix elements for the $j=0\rightarrow2$, $\nu=0\rightarrow1$ transitions from these data.

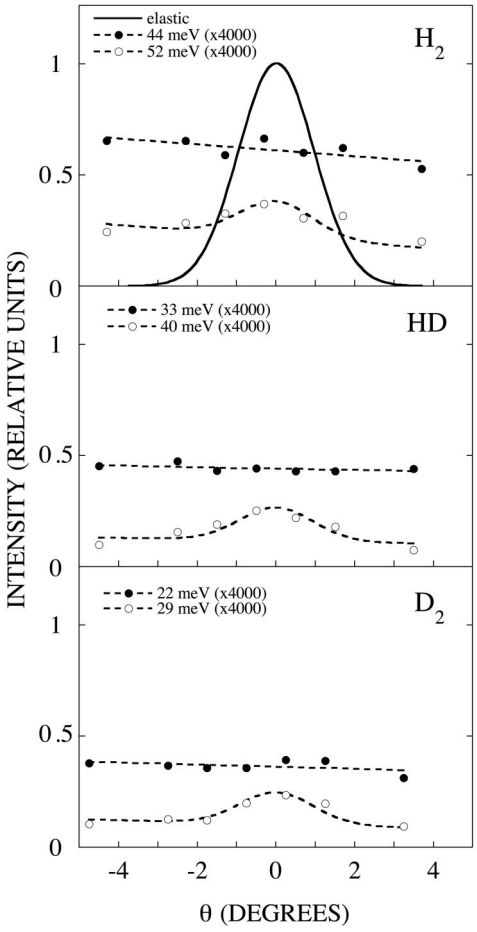

FIG. 2. Experimental elastic peak intensity (solid curve) and inelastic peak intensities versus collection angle θ ($\theta=0°$ specular $\theta<0°$ towards surface normal) for $j=0\rightarrow2$ (solid circles) and $j=0\rightarrow2, \nu=0\rightarrow1$ (open circles) excitations of H_2, HD, and D_2. Conditions as in Fig. 1.

The differential cross section for dipole scattering is, to a good approximation, given by[11]

$$\frac{d\sigma}{d\Omega}=n_s\left(\frac{me}{\pi\epsilon_0\hbar^2}\right)\mu_\nu^2\frac{\mathbf{k_1}}{\mathbf{k_0}}\frac{1}{\cos\theta_i}\frac{|\mathbf{k_1''}-\mathbf{k_0''}|^2}{|\mathbf{k_1}-\mathbf{k_0}|^4}, \tag{1}$$

where n_s is the number of adsorbed species per unit area, μ_ν is the dipole matrix element for a transition between states 0 and ν, whereas $\mathbf{k_0}$, $\mathbf{k_1}$, and $\mathbf{k_0''}$, $\mathbf{k_1''}$ are the wave vectors and their surface components of the incident and scattered electrons, respectively, and θ_i is the angle of incidence measured from the surface normal.

The EELS data reported in Figs. 1 and 2 were obtained for uncompressed physisorbed monolayers of H_2, D_2, and HD of approximately equal adsorbate density around 0.7×10^{15} molecules/cm^2. From the dipole contribution to the $j=0\rightarrow2$, $\nu=0\rightarrow1$ peaks in Fig. 2, we obtain the dipole matrix elements 5.6×10^{-3}, 5.7×10^{-3}, and 5.5×10^{-3} D [the unit is the Debye (D)] for H_2, HD, and D_2, respectively. For the $j=0\rightarrow2$ rotational transitions the dipole matrix elements must be less than $1-2\times10^{-3}$ D since we do not observe a distinct dipole contribution in the angular distributions.

We noted in Sec. I that H_2 and D_2 preferentially adsorb at Cu and Au adatoms deposited on the cold Cu(100) surface. He scattering experiments[1] show that rapid diffusion of Cu adatoms on Cu(100) only occur at temperatures above 300 K. Hence adatom diffusion on the 10 K Cu(100) surface is negligible and for small coverages the adatom distribution will be dominated by monomers. We judge, for the same reason, that diffusion of Au adatoms into the 10 K Cu(100) surface is highly improbable. We find that H_2 and D_2 bind more strongly at the adatoms than on the bare Cu(100) surface. Appropriate adsorption conditions were established at a specimen temperature and pressure where stable adsorption did not take place on the bare surface but only in the presence of deposited adatoms. At low adatom concentration, $<4\%$ of a monolayer, we detect approximately six adsorbed hydrogen molecules per adatom, which appears to be an optimal dense two dimensional configuration considering reasonable van der Waals bond lengths.

EELS measurements show that the molecules are physisorbed but with a characteristic signature: a distinct dipole activity of the $j=0\rightarrow 2$ rotational transition. Here we illustrate this effect for D_2 adsorbed at Au adatoms. The EELS spectra for D_2 adsorbed on the bare Cu(100) surface and at the Au adatoms show equal $j=0\rightarrow 2$ rotational and $j=0\rightarrow 2$, $\nu=0\rightarrow 1$ rotation-vibration features at 22 and 29 meV, respectively. While the $j=0\rightarrow 2$ rotational angular distribution for D_2 on Cu(100) is smooth and broad (see Fig. 2) and characteristic for short-range inelastic electron scattering, the corresponding distribution for D_2 at the Au adatoms, shown in Fig. 3, exhibits a dipole-excited specular peak superimposed on a broad short-range scattered background. The density of adsorbed D_2, 0.45×10^{15} molecules/cm^2, is obtained directly from the $j=0\rightarrow 2$ short-range rotational inelastic scattering intensity. This corresponds to approximately $2D_2$ molecules per Au adatom at this particular adatom concentration. From the dipole contribution to the $j=0\rightarrow 2$ rotational intensity in Fig. 3 and the surface density of D_2, we obtain, from Eq. (1), the dipole matrix element 8.5×10^{-3} D. Note that this value is even larger than the observed $j=0\rightarrow 2$, $\nu=0\rightarrow 1$ matrix element for D_2 on the bare Cu(100) surface.

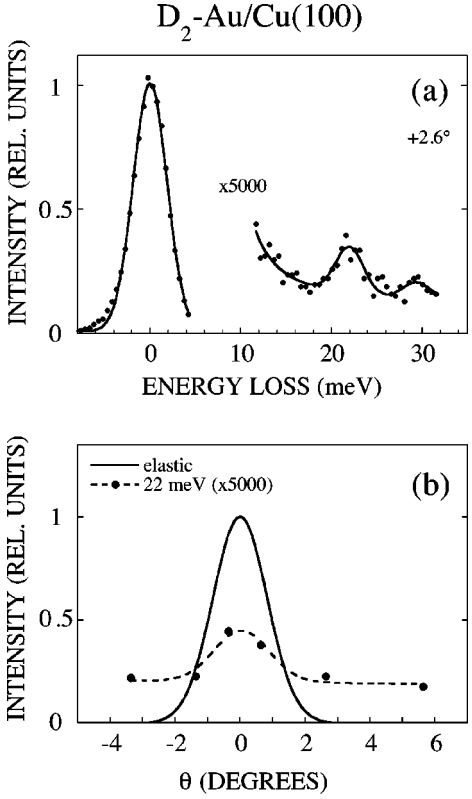

FIG. 3. (a) Off-specular (+2.6°) EELS spectrum of D_2 adsorbed at Au atoms on Cu(100), Au coverage 0.27×10^{15} atoms/cm^2. The elastic peak corresponds to specular scattering condition. (b) Corresponding elastic and inelastic peak intensity versus collection angle θ for the $j=0\rightarrow 2$ rotational excitation.

III. THEORY

Experimental and theoretical studies of physisorbed H_2 and D_2 molecules on low-index metal surfaces show that the physisorption affects the lateral and rotational motion, whereas the intramolecular vibrational motion is essentially unaffected. The isotopic molecules H_2 and D_2 have the same electronic configuration and experience the same physisorption interaction, which is composed of a van der Waals attraction and a Pauli repulsion due to the overlap of the electron densities of the metal and the molecule.[12,13] These two terms add up to give the laterally averaged isotropic interaction potential as

$$V_0(z) = V_R(z) + V_{vdW}(z), \tag{2}$$

where the repulsive and attractive terms are given by

$$V_R(z) = C_R e^{-\alpha z} \tag{3}$$

and

$$V_{vdW} = -C_{vdW}\frac{f_2(2k_c(z-z_{vdW}))}{(z-z_{vdW})^3}, \tag{4}$$

respectively. Here C_R describes the strength and α the inverse range of the repulsive potential, C_{vdW} is the strength of the van der Waals attraction, k_c is related to the inverse size of the molecule, and z_{vdW} is the position of the van der Waals reference plane. The damping factor $f_2(x)$ takes care of the singularity at z_{vdW}, and is described by

$$f_2(x) = 1 - \left(1 + x + \frac{x^2}{2}\right)e^{-x}. \tag{5}$$

In the case of physisorption of hydrogen on the Cu(100) surface, we use parameters from the literature,[14] namely, $C_R=5.21$ eV, $\alpha=1.24\ a_0^{-1}$, $C_{vdW}=4.74\ \text{eV}a_0^3$, $k_c=0.45\ a_0^{-1}$, and $z_{vdW}=0.563\ a_0$.

The interaction also depends on the angle θ between the surface normal and the molecular axis. This anisotropy is well described by the leading-order anisotropic term in an expansion of $V(z,\theta)$ in Legendre functions, given by

$$V(z,\theta) = V_0(z) + V_2(z)P_2(\cos\theta), \tag{6}$$

where $V_2(z)$ can be written as

$$V_2(z) = \beta_R V_R(z) + \beta_{vdW} V_{vdW}(z). \quad (7)$$

The anisotropy of the polarizability tensor for the free H_2 molecule gives $\beta_{vdW}=0.05$ on Cu(100),[15] while $\beta_R=-0.002$ was obtained from measured rotational substate splittings.[14]

The dipole matrix elements were obtained by the use of a numerical, pseudospectral wave-packet propagation method based on a discrete variable and finite basis representation (DVR-FBR) of the wave function.[16] The FBR is built up by a direct product of plane waves in the z coordinate and associated Legendre functions in the θ coordinate. Within the pseudospectral wave-packet method, the dipole matrix elements can be evaluated by studying the Fourier transform of the autocorrelation function. Here the autocorrelation function is obtained by the time evolution of an initial wave packet under the influence of a dipole function. The Fourier transform spectrum contains peaks at the positions of the eigenenergies if the transition is dipole active and the square-root of the area under each peak can be compared with the experimentally measured dipole matrix element. For the time propagation the standard split-operator approximation is used.[17] In this approximation, the potential-energy operator is evaluated in the DVR, the kinetic-energy operator is evaluated in the FBR, and the propagation of the wavefunction is performed by repeated transformations between the DVR and the FBR. The reason for the evaluation of the operators in the two different representations is that the potential-operator is local in the DVR, whereas the kinetic-operator is diagonal in the FBR with rotational energies given by the gas-phase values.[18]

IV. RESULTS AND DISCUSSION

The anisotropy of the interaction [see Eq. (7)] is dominated by the attractive part and hence by the anisotropy of the polarizability of the H_2 molecule. The anisotropic component $V_2(z)P_2(\cos\theta)$ of $V(z,\theta)$ gives rise to a coupling between the rotational motion and the vibrational motion in the potential well. The latter is dipole active and dipole transitions between the well states have been observed in EELS measurements.[9] As a consequence, the rotational motion will be dipole active. Furthermore the anisotropy of the electronic polarizability $\alpha(\theta)$ of the H_2 molecule will directly make the rotational motion dipole active.

It is not clear, as we have noted earlier,[6] how to calculate the dipole moment function for a physisorbed molecule in the spatial region of interest, where we have comparable contributions from both Pauli repulsion and van der Waals attraction. In particular, we have no detailed knowledge about the repulsive contribution. We found, however, that the measured dynamic dipole moments for the transitions among the well states of H_2 on Cu(100) can be reproduced by a simple phenomenological model for the dipole moment function, given by

$$\mu_R(z) = \mu_{R,0} e^{-\beta_0(z-z_0)}, \quad (8)$$

where z_0 is the position of the potential minimum and with parameters $\mu_{R,0}=0.051$ D and $\beta_0=0.9\ a_0^{-1}$. The basic idea for this form is that the overlap between a molecular orbital and the tail of a metal electron wave function decreases exponentially with z.

The polarization of the adsorbate due to the attractive van der Waals forces gives rise to an induced dipole,[2,3] which varies as z^{-4}. We find that the well state transitions can be reproduced by

$$\mu_{vdW}(z) = \frac{\mu_{vdW,0}}{(z/z_{vdW}-1)^4} f_3(x) \quad (9)$$

with parameters $\mu_{vdW,0}=57$ D and $z_{vdW}=0.7\ a_0$, $f_3(x)$ is a damping factor analogous to $f_2(x)$ in Eq. (5).

Considering the angular dependence of the van der Waals interaction via the electronic polarizability $\alpha(\theta)$, we have modified Eq. (9) to include a θ-dependent contribution in the prefactor, given by

$$\mu_{vdW}(z,\theta) = \frac{\mu_{vdW,0} + \mu_{vdW,2} P_2(\cos\theta)}{(z/z_{vdW}-1)^4} f_3(x). \quad (10)$$

Tentatively, we relate the term $\mu_{vdW,0}+\mu_{vdW,2}P_2(\cos\theta)$ to $\alpha(\theta)$ as

$$\alpha(\theta) = \alpha_0 + \alpha_2 P_2(\cos\theta), \quad (11)$$

thus $\mu_{vdW,2}/\mu_{vdW,0}=\alpha_2/\alpha_0$ where α_0 and α_2 are given by[15]

$$\alpha_0(\theta) = \frac{1}{3}(\alpha_L + 2\alpha_T), \quad \alpha_2(\theta) = \frac{1}{6}(\alpha_L - \alpha_T). \quad (12)$$

Here α_L and α_T are the components of the polarizability tensor along and normal to the axis of the molecule and values[19] for free H_2 give $\alpha_0=5.3\ a_0^3$ and $\alpha_2=0.25\ a_0^3$. Hence, for $\mu_{vdW,0}=57$ D, we get $\mu_{vdW,2}=2.8$ D. We note that there may also be an anisotropic contribution to the dipole function in Eq. (8) related to the anisotropy of the repulsive interaction. We will discuss this effect below.

Using the dipole functions in Eqs. (8)–(10) and the values for $\mu_{R,0}$, β_0, $\mu_{vdW,0}$, z_{vdW}, and $\mu_{vdW,2}$, we have calculated the dipole spectral function $C_\mu(\omega)$ for H_2 and D_2, respectively, following our previous scheme.[6] The dipole matrix elements $|\langle\nu|\mu|0\rangle|$ for vibrational excitations in the potential well were accurately reproduced. Figure 4 shows an example of a calculated dipole spectral function, $C_\mu(\omega)$, for H_2 on Cu(100) using Eq. (10) and the relevant parameters given above. The sharp peaks correspond to transitions from the ground state to the $j=2$ rotational state and its combinations with the $\nu=1$ and $\nu=2$ vibrational states. Calculated dipole matrix elements for the rotation and the rotation-vibration combination mode, $|\langle\nu,j|\mu|0,0\rangle|$ for H_2 and D_2 on Cu(100) are listed in Table I together with the experimental data which include estimated upper bounds for pure rotations. Note that it is only the $m=0$ component of the (j,m) substates that is dipole active since the interaction only depends on θ. Comparison between calculated and measured data reveal several interesting features: (i) The calculated values for the rotation-vibration modes are much smaller than the experimental values. (ii) Including the anisotropic polarizability term $\mu_{vdW,2}P_2(\cos\theta)$ in $\mu_{vdW}(z,\theta)$ increases the calculated values substantially but they are still about an order of magnitude smaller than the measured ones. (iii) The calculated values

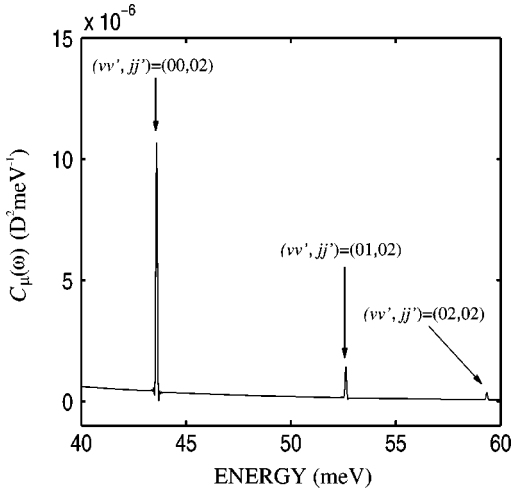

FIG. 4. The calculated dipole spectral function for H_2 on Cu(100) obtained from Eq. (10). The peaks occur for any dipole active transition between the eigenstates in the physisorption potential, and the square-root of the area under each of these peaks is the calculated value of the dipole matrix element. The unit is Debye.

for the pure rotational transition, $|\langle 0,2|\mu|0,0\rangle|$, are, for these dipole functions, larger than the values for the rotation-vibration transition, $|\langle 1,2|\mu|0,0\rangle|$, while the measured data show the opposite trend.

The dipole matrix elements associated with the coupling between rotational and vibrational motion via $V(z,\theta)$ [see Eqs. (6) and (7)] are clearly very weak for both $\mu_R(z)$ and $\mu_{vdW}(z)$. Appreciable rotational dipole strength is observed only when the anisotropic term $\mu_{vdW,2}P_2\cos\theta$ is included in $\mu_{vdW}(z,\theta)$. However, as we noted above, the calculated values for the rotation-vibration modes are much smaller than the observed values resulting in a wrong trend of the relative dipole strengths. This aspect indicates that our model lacks an essential ingredient of the dipole moment function. For this reason, we also investigated a θ-dependent contribution to the phenomenological dipole function μ_R. Such a contribution may derive from the angular dependence of the overlap of the molecule and metal electron densities. We modified Eq. (8) to include a θ-dependent contribution

$$\mu_R(z,\theta) = [\mu_{R,0} + \mu_{R,2}P_2(\cos\theta)]e^{-\beta_0(z-z_0)} \qquad (13)$$

The parameter values $\mu_{R,0}$ and β_0 were kept the same as above; i.e., $\mu_{R,0}=0.051$ D and $\beta_0=0.9a_0^{-1}$. For $\mu_{R,2}=0.0024$ D, which corresponds to the anisotropy of $\mu_{vdW}(z,\theta)$, we obtain, for H_2, the values 0.87×10^{-3} D and 0.35×10^{-3} D for the rotation and rotation-vibration matrix elements, respectively. These values are very close to those we obtained for $\mu_{vdW}(z,\theta)$ as can be seen in Table I and the differences with respect to the measured data are the same for $\mu_R(z,\theta)$ and $\mu_{vdW}(z,\theta)$. We have found that this also holds for a combined dipole moment function

$$\mu(z,\theta) = \mu_R(z,\theta) + \mu_{vdW}(z,\theta) \qquad (14)$$

Depending on the relative signs of $\mu_{R,2}$ and $\mu_{vdW,2}$ the rotation and rotation-vibration matrix elements either increase or decrease, but their relative strengths remain essentially as for the two components; i.e. opposite to the measured trend.

In Sec. II we presented experimental data for D_2 physisorbed at Au atoms on the Cu(100) surface, which revealed a significant dipole activity of the $j=0\rightarrow2$ rotational transition at 22 meV. The measured dipole matrix element is 8.5×10^{-3} D, which is much larger than the estimated upper bound observed for D_2 on Cu(100) and an order of magnitude larger than the value, 0.81×10^{-3} D, calculated for D_2 on Cu(100) from Eq. (10) (see Table I) for the van der Waals induced dipole. Part of the large difference between theory and experiment can be sorted out in a straightforward manner. Only the $m=0$ component of the $j=0\rightarrow2$ rotational multiplet is dipole active for D_2 on the bare Cu(100) surface. When the molecule is adsorbed at the Au adatom this condition breaks down and all five m-substates become dipole active. These contribute equally to the measured signal so the relevant measured value to compare with is $8.5/\sqrt{5}=3.8\times10^{-3}$ D. This is still substantially larger than the calculated value for D_2 on Cu(100) and the interaction with the neighboring Au adatom evidently contributes in an important way to the rotational dipole activity of the molecules adsorbed at the adatoms.

V. CONCLUSIONS

We have measured the dipole activity of rotation and rotation-vibration modes for hydrogen molecules physisorbed on the bare Cu(100) surface and at Au adatoms on the same surface. We find in our calculations for the bare Cu(100) case, using a van der Waals dipole function and an exponentially decaying dipole function only weak dipole activity linked to the coupling between rotational and vibrational motion in the potential well. The anisotropy of the molecular electronic polarizability, on the other hand, affects

TABLE I. Dipole matrix elements $|\langle\nu,j|\mu|0,0\rangle|$ for hydrogen molecules adsorbed on the Cu(100) surface. Here ν and j represent vibrational and rotational quantum numbers, respectively. Values denoted by (a) are obtained by the use of the dipole function in Eq. (8), (b) comes from Eq. (9), and (c) is obtained from Eq. (10). The unit is the Debye.

	H_2				D_2			
ν,j	Expt.	Calc.[a]	Calc.[b]	Calc.[c]	Expt.	Calc.[a]	Calc.[b]	Calc.[c]
0,2	$<2\times10^{-3}$	0.11×10^{-3}	0.19×10^{-3}	0.87×10^{-3}	$<2\times10^{-3}$	0.3×10^{-3}	0.26×10^{-3}	0.83×10^{-3}
1,2	5.7×10^{-3}	0.07×10^{-3}	0.10×10^{-3}	0.27×10^{-3}	5.2×10^{-3}	0.18×10^{-3}	0.13×10^{-3}	0.22×10^{-3}

the van der Waals induced dipole directly and causes significant dipole activity of the pure rotations but relatively weak activity of the rotation-vibration modes. The experimental data for hydrogen molecules on Cu(100) show the opposite trend, which indicates that our dipole moment function lacks an essential ingredient. The measured rotational dipole activity for H_2 and D_2 physisorbed at Au adatoms on Cu(100) is much larger than the values calculated for the bare Cu(100) surface. Part of this can be explained by the different (j,m) selection rules operating in the two cases. It is clear, however, that the proximity to the Au adatom is an important factor contributing to the induced dipole activity.

ACKNOWLEDGMENTS

We thank M. Persson for useful comments about this work. Financial support from the Swedish Science Council and the Swedish Foundation for Strategic Research (SSF) via Materials Consortia No. 9 and ATOMICS, is gratefully acknowledged.

[1] J. Bellman, Ph.D. thesis, Department of Applied Physics, Chalmers University of Technology and Göteborg University, Göteborg, Sweden, 2004.
[2] P. R. Antoniewicz, Phys. Rev. Lett. **32**, 1424 (1974).
[3] E. Zaremba, Phys. Lett. **57A**, 156 (1976).
[4] G. Herzberg, *Spectra of Diatomic Molecules* (Van Nostrand, New York, 1950).
[5] J. Heidberg, M. Vossberg, M. Hustedt, M. Thomas, S. Briquez, S. Picaud, and C. Girardet, J. Chem. Phys. **110**, 2566 (1999).
[6] M. Hassel, K. Svensson, J. Bellman, S. Andersson, and M. Persson, Phys. Rev. B **65**, 205402 (2002).
[7] S. Andersson in *Vibrations at Surfaces*, edited by R. Caudano, J. M. Gilles, and A. A. Lucas (Plenum, New York, 1982) p. 169; K. Svensson, Ph.D. thesis, Department of Applied Physics, Chalmers University of Technology and Göteborg University, Göteborg, Sweden, 1997.
[8] L. Wilzén, S. Andersson, and J. Harris, Surf. Sci. **205**, 387 (1988).
[9] K. Svensson and S. Andersson, Phys. Rev. Lett. **78**, 2016 (1997).
[10] K. Svensson and S. Andersson, Surf. Sci. **392**, L40 (1997).
[11] B. N. J. Persson, Solid State Commun. **24**, 573 (1977).
[12] P. Nordlander, C. Holmberg, and J. Harris, Surf. Sci. **152**, 702 (1985).
[13] A. Chizmeshya and E. Zaremba, Surf. Sci. **268**, 432 (1992).
[14] L. Wilzén, F. Althoff, S. Andersson, and M. Persson, Phys. Rev. B **43**, 7003 (1991).
[15] J. Harris and P. J. Feibelman, Surf. Sci. **115**, L133 (1982).
[16] R. Kosloff in *Time-Dependent Quantum Molecular Dynamics*, edited by J. Broeckhove and L. Lathouwers (Plenum, New York, 1992).
[17] M. D. Feit, J. A. Fleck, and A. Steigler, J. Comput. Phys. **47**, 412 (1982).
[18] K. P. Huber and G. Herzberg, *Molecular Spectra and Molecular Structure* (Van Nostrand, New York, 1979).
[19] Landolt-Börnstein, *Zahlen-werten und Functionen*, Vol. I, part 3, p. 510 (Springer, Berlin, 1951).